RELATIONSHIP BETWEEN THRESHOLD PORE SIZE AND AIR PERMEABILITY, WATER PERMEABILITY, AND GAS PERMEATION

Y. SAKAI[1*†], C. NAKAMURA[2], and T. KISHI[1]

[1] *Institute of Industrial Science, The University of Tokyo, Japan*
[2]*Graduate School of Engineering, The University of Tokyo, Japan*

ABSTRACT

This paper shows that not only air and water permeability, but also gas permeation through concrete can be evaluated with threshold pore radius. The authors have proposed a new method to measure threshold pore size of concrete. Samples for MIP analysis were coated with epoxy putty and the pore radius corresponds to the maximum slope of the obtained cumulative pore size distribution is defined as threshold pore radius. Threshold pore radius obtained with the new method showed good correlation with surface air permeability and water permeability. Gas permeation was plotted on two lines against threshold pore size and the point of intersection between the two lines agreed with theoretical transition zone of diffusion. The obtained results indicated that threshold pore size governs various mass transfer such as air permeability, water permeability, and gas permeation.

Keywords: Threshold pore radius, surface air permeability, water permeability, gas permeation.

1. INTRODUCTION

Offending agents for concrete structures such as chloride ion, liquid water, CO2, etc. penetrate into concrete through pore network, so it is probable that resistivity against those agents can be evaluated based on concrete pore structure quantitatively. The relationship between pore structure and mass transfer resistance, however, is not understood enough for the evaluation. The authors have focused on threshold pore of concrete, developed a new method to evaluate it, and reported good correlation with air and water permeability (SAKAI et al., 2012). In this paper, the relationship between threshold pore size and gas permeation behavior is discussed.

2. DISCUSSION ON THE RELATIONSHIP BETWEEN THRESHOLD PORE SIZE AND AIR/ WATER PERMEABILITY

So far, many researchers have pointed out that there is good correlation between threshold pore size and air and water permeability. Powers (1958) and Mehta (1980) studied relationship between pore structures and water permeability. Powers found correlation between volume of capillary pore and

---

* Corresponding author: Email: ysakai@iis.u-tokyo.ac.jp

† Presenter: Email: ysakai@iis.u-tokyo.ac.jp

water permeability, and Metha reported a good correlation between threshold pore size and water permeability. Here, threshold pore size is the minimum pore size which mass should pass to penetrate the objective, and pore size distribution is measured with Mercury Intrusion Porosimetry (MIP). Halamickova and Detwiler (1995) reported that there was a correlation between critical pore size, an indicator of pore structure, and both water permeability and coefficient of oxygen diffusion. Goto (1996) related threshold pore size with hydration rate of cement. The indicators of pore structures and permeability shown above, however, can't show such high correlation in various types of specimens since it is not easy to extract threshold pore size correctly, particularly, in samples taken from concrete specimens.

The authors (Sakai et al., 2012) have proposed a new method to extract the threshold pore size by using epoxy-putty-coated specimen in MIP. Here, the definition of threshold pore size is following Winslow and Diamond (1970), the corresponding pore size where cumulative pore size distribution shows the largest tangent. In our method, 5mm cubic piece of sample is coated with epoxy putty leaving a small area of around 4 mm^2, and analyzed with MIP (Figure 1). The epoxy putty is dried for 72 hours after application. The expected effect of coating is as follows; in normal sample, mercury tries to avoid smaller pores, including threshold pore, and, as a result, large part of the sample is already filled when mercury starts intruding into threshold pore (Figure 2(a)). On the

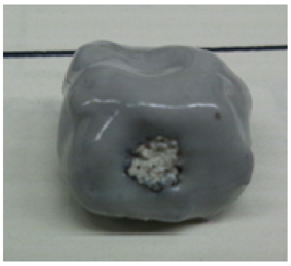

Figure 1: Epoxy-coated sample

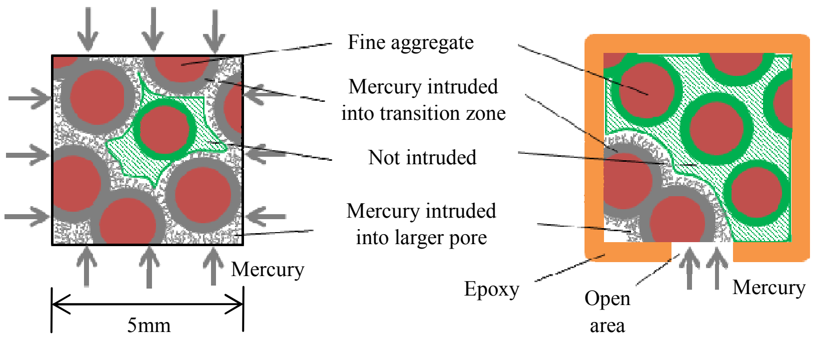

(a)Normal sample

(b)Epoxy-coated sample

Figure 2: Schematic view of mercury intrusion with/without coating

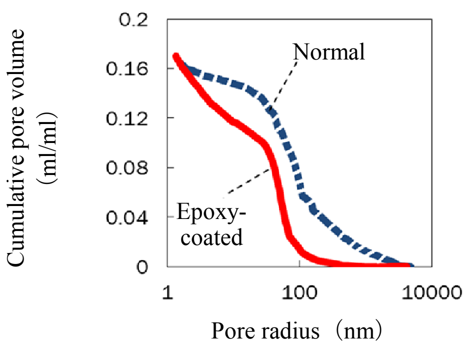

Figure 3: Example of measured pore radius distribution of mortar sample taken from concrete

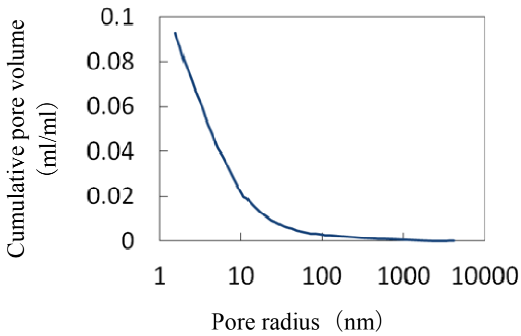

Figure 4: Measured pore radius distribution of epoxy putty cube

other hand, when coating is applied to the sample, because of the limited open area, mercury can't avoid the smaller pore and less intrusion occur until it reaches threshold pore size (Figure 2(b)), followed by sudden intrusion. Figure 3 is an example of measured pore radius distribution. It is clear that epoxy-coated specimen, shown in solid line, has clearer sudden intrusion compared with normal specimen, broken line. It is already confirmed that sudden intrusion occurs at the obtained threshold pore radius with epoxy-coated specimen by observing the split surface of specimens (SAKAI, 2012). Figure 4 is measured pore radius distribution of hardened epoxy putty of 5mm cubic piece. The result shows that epoxy-coating affects the measured result when mercury is intruded below 10nm.

The correlation between threshold pore radius and surface air permeability (Torrent method) and water permeability was examined with concrete specimen of various mixing design and curing

Table 1 Mix proportion of concrete

Name	W/B (%)	Curing	Mass per unit volume（kg/m^3）					AE water reducing agent	AE agent
			W	C	FA or BFS	S	G		
N40-1	40	Water	180	450	-	708	978	C×0.20%	C×0.004%
N55-1	55	Water	180	327	-	805	984	C×0.20%	C×0.004%
N70-1	70	Water	180	257	-	886	960	C×0.20%	C×0.004%
FB55-1	55	Water	172	251	62	791	1007	C×0.20%	C×0.004%
FC55-1	55	Water	169	216	92	783	1017	C×0.20%	C×0.004%
BA55-1	55	Water	179	260	65	787	1002	C×0.20%	C×0.004%
BB55-1	55	Water	174	159	159	792	1008	C×0.20%	C×0.004%
N70-3	70	Wind	180	257	-	886	960	C×0.20%	C×0.004%
FB40-1	40	Water	172	345	86	694	998	C×0.20%	C×0.004%
FB70-3	70	Wind	172	197	49	873	985	C×0.20%	C×0.004%
BB40-1	40	Water	174	218	218	695	1001	C×0.20%	C×0.004%
BB70-3	70	Wind	174	124	124	873	985	C×0.20%	C×0.004%
L55-2	55	Sealed	180	327	-	807	987	C×0.15%	C×0.006%
M55-2	55	Sealed	180	327	-	807	987	C×0.15%	C×0.006%
H55-2	55	Sealed	180	327	-	804	984	C×0.25%	C×0.002%

Table 2 Concrete properties of existing structure members

Member	Design strength(MPa)	W/C (%)	Mass per unit volume（kg/m^3）				
			W	C	S	G	Water reducing agent（%/C）
Railing	24	48	165	348	851	936	0.22
Abutment	24	50	175	353	757	1025	0.30
Pear	24	50	175	353	757	1025	0.30
Pavement	27-30	42	144	340	682	1192	0.15

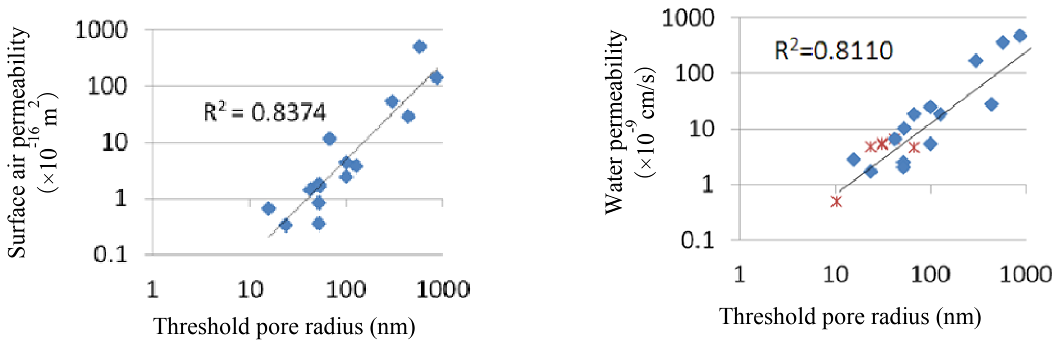

(a)Surface air permeability (b)Water permeability

Figure 5: Threshold pore radius and surface air and water permeability (Quarry: Specimens prepared in lab., Asterisk: Core samples)

condition as shown in Table 1. OPC (N), low-heat cement (L), moderate-heat cement (M), and high early strength cement (H) are used. Number in specimen's name before and after hyphen indicates water-to-binder ratio and curing condition, respectively. Specimens were demolded 24 hours after the casting and under-water, sealed, or in-wind curing were given until the age of 28 days, and after that, all specimens were cured in a room of 20 degree Celsius. Here, in in-wind curing, specimens are winded by a fan to accelerate drying. All tests were conducted when the age of the specimens were 2.75 years. Core samples taken from existing structures were also analyzed. The concrete properties of the members are shown in Table 2, and the age of the members are around 11 years. It was confirmed that the threshold pore size, obtained by the new method, and air and water permeability showed good correlation as shown in Fig. 5. The good correlation indicates that threshold pore governs air and water permeation and chemical property of concrete affect less to above permeation behavior.

3. THRESHOLD PORE SIZE AND GAS PERMEATION

3.1. MEASURING SETUP AND PROCEDURE

Specimens used in the previous chapter were used to study nitrogen gas penetration. After water permeation test, the specimens had been dried in room of 20 degree Celsius for six months. Specimens were put on a container filled with nitrogen gas, as shown in Figure 6, and oxygen concentration in a container put on the specimen was measured to evaluate nitrogen permeation through the specimen. The side of the specimens was covered with aluminum tape and gap between specimen and container was filled with denture adhesive to avoid the influx of air. After the test, air permeability of the specimens was measured with Torrent method. FB40-1 of different thickness, 38mm, 15mm, and 5mm was also tested.

3.2. TEST RESULTS

The reduction of oxygen concentration and the time after the reduction starts is shown in Figure 7. The concentration decreases almost linearly and the reduction rate changes much depending the mix proportion of concrete and curing condition. Hereinafter, the tangents of the lines in Figure 7 are called nitrogen permeation rate. The relationship between nitrogen permeation rate and threshold pore radius is shown in Figure 8. Here, threshold pore radius is converted from surface air permeability with the regression expression, equation (1), as lined in Figure 5(a).

$$Threshold\ \ pore\ radius\left(nm\right)=46\times\sqrt{Surface\ \ air\ \ permeability\ kT\ \left(\times10^{-16}\ m^{2}\right)} \tag{1}$$

It is clear that the plots distributes on two lines of different slope, in other words, with larger threshold pore radius than 100nm, nitrogen permeation rate is almost flat, however, with threshold pore radius smaller than 100nm, the rate drops as the pore radius decreases. When the pore radius is enough large, gas diffusion is governed by molecular diffusion. As the radius become smaller, the collision rate between molecular and wall become higher, and Knudsen diffusion become dominant. The above diffusion coefficients are expressed as equation (2) and equation (3) (Takeuchi 1999).

$$D_M=\frac{0.001858\sqrt{T^3(M_1+M_2)/M_1M_2}}{P\sigma_{12}^2\Omega_D} \tag{2}$$

$$D_K=9700r\sqrt{\frac{T}{M}} \tag{3}$$

Here, D_M: molecular diffusion coefficient (cm2/s), D_K: Knudsen diffusion coefficient(cm2/s), T: absolute temperature(K), M: Molar weight, P: total pressure (atm), σ: collision diameter($\times10^{-10}$m), Ω_D: collision integral, r: pore radius(cm). Total diffusion coefficient is expressed as equation (4).

$$\frac{1}{D}=\frac{1}{D_M}+\frac{1}{D_K} \tag{4}$$

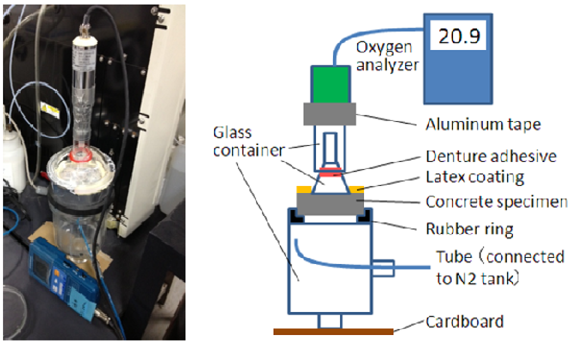

Figure 6: Schematic view of measurement

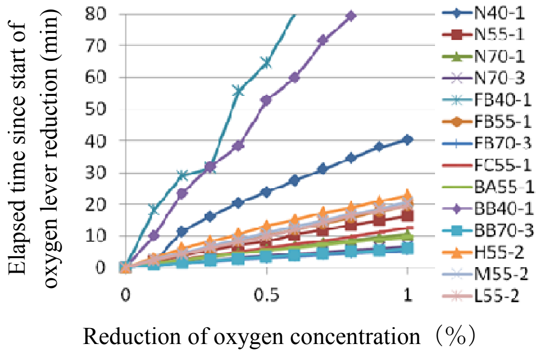

Figure 7: Reduction of oxygen concentration and elapsed time since start of reduction

Ω_D is obtained from equation (5) (Ohe 2002; Neufeld et al.1972).

$$\Omega_D = \frac{A}{T^{*B}} + \frac{C}{\exp DT^*} + \frac{E}{\exp FT^*} + \frac{G}{\exp HT^*} \tag{5}$$

Here, $T^*=kT/\varepsilon$, k: Boltzmann constant, ε: maximum attractive energy, A-H: constant (A=1.06036, B=0.15610, C=0.19300, D=0.47635, E=1.03587, F=1.52996, G=1.76474, H=3.89411). Using the condition of the experiment (T=293K, M=28, P=1atm, σ=0.35nm, ε/k=71.4) (Ohe 2002; Svehla 1962), D is calculated and shown in Figure 9 against r. As with Figure 8, diffusion coefficient is almost flat above 100nm, and decreases below it. The inflection point agreed well between measured and theoretical value, around 100nm. FB40-1 of 38mm thick is the left-below−most triangle plot and FB40-1 of 15mm and 5mm thick are solid circle plots. The figure shows that even the specimen thickness is different, the results are plotted on same lines and as the specimen thickness decreases, threshold pore radius increases. The results show that gas permeation through concrete is governed by threshold pore because, according to the definition, it is the minimum pore which mass have to pass through to penetrate and threshold pore worked as a bottleneck which controls the diffusion rate. The above results indicate that in concrete also, if the pore size is smaller than a certain size, diffusion rate decreases, and converted threshold pore size from surface air permeability corresponds to the pore size which governs gas diffusion in concrete.

4. CONCLUSIONS

The authors have proposed a new method to measure threshold pore size of concrete. Samples for MIP analysis were coated with epoxy putty and the pore radius corresponds to the maximum slope of the obtained cumulative pore size distribution is defined as threshold pore radius. Threshold pore radius obtained with the new method showed good correlation with surface air permeability and water permeability. Gas permeation rate was measured and obtained results distributed on two lines against threshold pore size. The point of intersection between the two lines agreed with theoretical transition zone of diffusion. The obtained results indicated that threshold pore size governs various mass transfer such as air permeability, water permeability, and gas diffusion rate.

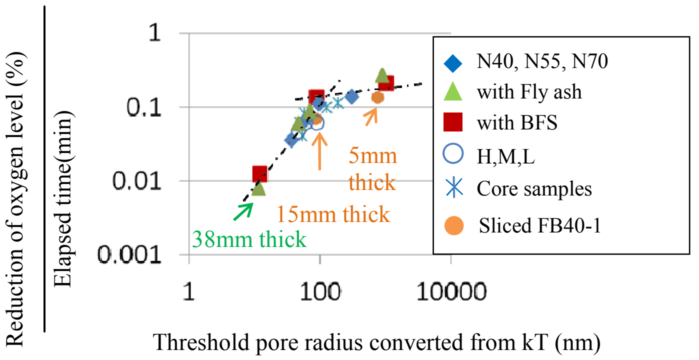

Figure 8: Reduction rate of oxygen level and threshold pore radius converted from kT

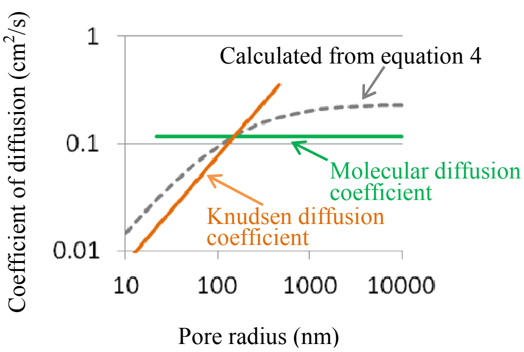

Figure 9: Molecular diffusion and Knudsen diffusion

REFERENCES

Goto T (1996). Modeling of cement haydration reaction and strength development. Ph. D. thesis. the University of Tokyo.

Halamickova P and Detwiler R (1995). WATER PERMEABILITY AND CHLORIDE ION DIFFUSIONIN PORTLAND CEMENT MORTARS: RELATIONSHIP TO SAND CONTENT AND CRITICAL PORE DIAMETER. Cement and Concrete Research. 25(4). pp. 790-802.

Mehta P and Manmohan D (1980). Pore size distribution and permeability of hardened cement paste. 7th International Congress Chemistry of Cement, Paris. Vol. 3. pp.71-75.

Nakamura C, Sakai Y, and Kishi T (2012). Study on the effects of chemical and physical properties of concrete on the behavior of internal water. Proceedings of 11th International Symposium on New Technology for Urban Safety of Mega Cities in Asia.

Neufeld PD, Janzen AR, and Aziz RA (1972). Empirical equations to calculate 16 of the transport collision integrals Ω for the Lennard-Jones potential. the journal of chemical physics. 57(3).

Ohe S (2002). Estimation method of physical property (in Japanese). Data book publisher.

Powers T (1958). The Physical Structure and Engineering Properties of Concrete. Research and Development. Bulletin of Portland Cement Association. No. 90.

Sakai Y, Nakamura C, Kishi T, and Ahn T (2012). Interpretation of Non-Destructive Test Results for Evaluation of Mass Transfer Resistance of Concrete Members. the 5th International Conference of Asian Concrete Federation.

Svehla RA (1962). Estimated Viscosities and Thermal Conductivities of Gases at High Temperatures. NASA technical report R-132, Lewis Research Center.

Winslow D and Diamond S (1970). A mercury porosimetry study of the evolution of porosity in Portland cement. Journal of Materials. Vol. 5, pp. 564-585.